



# INTERNATIONAL JOURNAL OF ADVANCE RESEARCH, IDEAS AND INNOVATIONS IN TECHNOLOGY

ISSN: 2454-132X

Impact factor: 4.295

(Volume 4, Issue 4)

Available online at: [www.ijariit.com](http://www.ijariit.com)

## Optimization of large size fabricated Y-Strainers for improvement in pressure drop value using CFD analysis

Sumit Shinde

[slshinde298@gmail.com](mailto:slshinde298@gmail.com)

Yadavrao Tasgaonkar College of Engineering and Management, Karjat, Maharashtra

Santosh Wankhede

[srw2008@rediffmail.com](mailto:srw2008@rediffmail.com)

Yadavrao Tasgaonkar College of Engineering and Management, Karjat, Maharashtra

### ABSTRACT

*In this project, a Y type strainer is considered for analysis. The design is an important industrial activity which influences the quality of the product. The strainer is modeled by using modelling software SolidWorks. By using this software, the time spent in producing the complex 3-D models and the risk involved in the design and manufacturing process can be easily minimized. So, the modelling of the strainer is to be made by using SolidWorks. Later this SolidWorks model will be imported to ANSYS for analysis work. ANSYS is the latest software used for simulating the different forces, the pressure acting on the component and also calculating and viewing the results. By using ANSYS software reduces the time compared with the method of mathematical calculations by a human. Studies on flow behavior in strainer have led to a continued effort on optimizing the strainer design. 3D, steady, incompressible, turbulent  $k-\epsilon$  Navier Stokes equations are solved numerically to predict the flow behavior and flow coefficient. CFD helps in the design optimization process with better accuracy and a considerable reduction in design lead time. The present work aims to study the effect of pressure drop and flow behavior across different strainer design. Based on the baseline simulation results, the optimized design is suggested. The calculated pressure drop for the optimized design shows 75% improvement compared to baseline design.*

**Keywords**— CFD, Strainer, Modeling, ANSYS

### 1. INTRODUCTION

In liquid filtration, the suspension passes through a filtration membrane; the suspended particles remain on its surface and in its pores, while the clarified liquid, called filtrate, is collected behind the filtration membrane (Screen). The separated solid phase, the sediment, forms a continuously growing layer on the filtration membrane surface. It commonly consists of randomly lying particles of different shapes.

In filters, a pressure drop occurs due to the screen placed inside the filter for contamination retention purpose. It is also called a screen. For Y type strainers this screen is made out of a combination of wire mesh and perforated sheet.

### 1.1 Analysis work & product development

Selecting the right techniques/process to incorporate into new products is a particularly challenging aspect of new product definition and development. While newer advanced technologies may offer improved performance, they also make the product development process more risky and challenging. In this project, we focus on the technical selection and commitment. For technical selection following process shall be followed.

- Selection of the filtration (mesh)
- Free flow area Calculation
- Pressure drop calculation

**Selection of the filtration (mesh):** Filtration Mesh is the heart of the strainer system and also some selection parameters are explained. One of the most important design considerations when purchasing a strainer is specifying the perforation or mesh size of the straining element. The straining element is a mechanical filter which removes and retains particles too large to pass through yet allows the flowing media (liquid or gas) to pass unobstructed. By cleaning the flowing media, the straining element helps to protect expensive downstream equipment such as pumps, meters, spray nozzles, compressors, and turbines.

**Determining Opening Size:** In general, screen openings should be approximately one-half the diameter of the largest allowable particle. The largest allowable particle is defined as the size of particle that can pass through downstream equipment without causing damage. For example, if the maximum allowable particle is 1/16 inch than the screen opening would be specified at 1/32 inch. In addition to the size of particles, the quantity of debris in the flowing media must also be considered when determining the appropriate opening size. Straining elements can only be used to remove insoluble floating impurities. The most common range of particle retention is 40 Mesh (0.5mm opening) for the Y-type strainer.

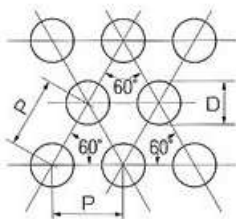
Remember the principle: “Not as fine as possible, but as fine as necessary.”

A common mistake is to specify a screen opening that is too small for the application. This can lead to overstraining and should be avoided for the following reasons:

- Maintenance costs are significantly increased due to excessive cleaning requirements.
- Pressure drop is increased dramatically.
- The straining element may become damaged and fail.

**Perforated Sheet:** Perforated sheet, also known as perforated metal, perforated plate, or perforated screen, is sheet metal that has been manually or mechanically stamped or punched to create a pattern of holes, slots, or decorative shapes. Materials used to manufacture perforated metal sheets include stainless steel, cold rolled steel, galvanized steel, brass, aluminum, tinplate, copper, Monel, Inconel, titanium, plastic, and more. This perforated sheet is used here to support fine wire mesh to withstand against the flow pressure.

**Calculation for an open area of perforated sheet:** Here in this project, the perforated sheet used is of Round Perforation - 60 Degree Staggered.  
 Hole Diameter (D) = 19mm  
 Pitch (P) = 22mm



$$\text{Opening Area} = 0.91 \left(\frac{D}{P}\right)^2 \quad (1)$$

$$\text{Opening Area} = 0.91 \left(\frac{19}{22}\right)^2 \quad (2)$$

$$\text{Opening Area} = 0.67$$

$$\text{Opening Area} = 67\%$$

**Wire mesh:** A mesh is a barrier made of connected strands of metal, fiber, or other flexible or ductile materials. A mesh is similar to a web or a net in that it has many attached or woven strands. Industrial wire cloth can be produced in many thousands of combinations of size and shape of opening, wire diameter, type of weave, and metal. Figure 3.1.2 shows typical plain wire mesh.

Wire mesh with size having 40Mesh 39SWG is used for analysis.

Mesh (n) = 40

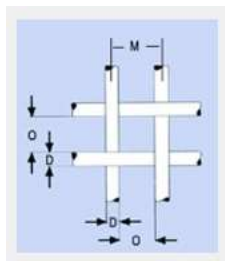
Wire Diameter (Dw) = 0.321mm

Pitch (M) =  $\frac{25.4}{n} = 0.635$

Opening (O) =  $M \times D = 0.5029$

Open area ( $d_s$ ) =  $\left(\frac{O}{M}\right)^2 = 0.627 \quad (2)$

% Open area of wire mesh = 62.7%



**Pressure drop:** Pressure drop is defined as the difference in total pressure between two points of a fluid carrying network. A pressure drop occurs when frictional forces, caused by the resistance to flow, act on a fluid as it flows through the tube. The main determinants of resistance to fluid flow are fluid velocity through the pipe and fluid viscosity. Pressure drop increases proportionally to the frictional shear forces within the piping network. A piping network containing a high relative roughness rating as well as many pipe fittings and joints, tube convergence, divergence, turns, surface roughness and other physical properties will affect the pressure drop. High flow velocities and/or high fluid viscosities result in a larger pressure drop across a section of pipe or a valve or elbow. Low velocity will result in lower or no pressure drop.

The pressure drop for incompressible flow across a screen of fractional free area  $\alpha$  may be computed from, (Reference: Perry Chemical hand Book, Section-6: Fluid and Particle Dynamics)

$$\Delta P = k \frac{\rho v^2}{2} \quad (3)$$

Where,  $\rho$  = Fluid density

$v$  = superficial velocity based upon the gross area of the screen

$k$  = Velocity head loss

$$k = \left(\frac{1}{C^2}\right) \left(\frac{1 - \alpha^2}{\alpha^2}\right) \quad (4)$$

The C with an aperture (ds) is given as a function of screen Reynolds number  $Re = D_s (V/\alpha)\rho/\mu$  in Fig. 1 for plain square-mesh screens,  $\alpha = 0.14$  to 0.79. This curve fits most of the data within  $\pm 20\%$ . In the laminar flow region,  $Re < 20$ , the discharge coefficient can be computed from

$$C = 0.1\sqrt{Re} \quad (5)$$

Coefficients greater than 1.0 in Figure 1 probably indicate partial pressure recovery downstream of the minimum aperture, due to rounding of the wires. Grootenhuis (Proc. Inst. Mech. Eng. [London], A168, 837–846 [1954]) presents data which indicate that for a series of screens, the total pressure drop equals the number of screens times the pressure drop for one screen, and is not affected by the spacing between screens or their orientation with respect to one another, and presents a correlation for frictional losses across plain square-mesh screens and sintered gauzes.

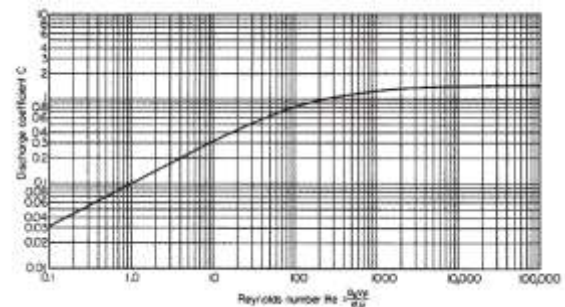


Fig. 1: Screen discharge coefficients, plain square-mesh screens. (Courtesy of E. I. du Pont de Nemours & Co.)

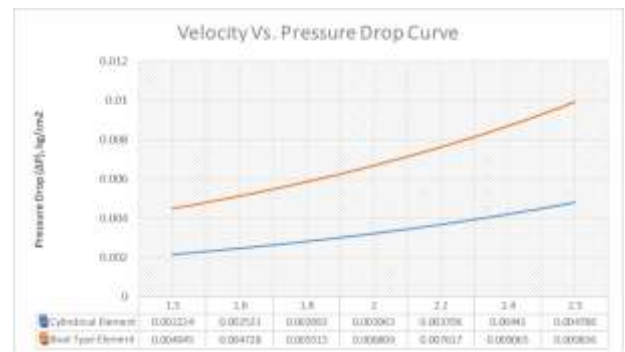


Fig. 2: Velocity vs. pressure drop curve

This achieved pressure drop value is for a filter element made of a combination of wire mesh and perforated sheet without any boundary condition. Here if we compare the results of both type of element it is found that cylindrical type element has minimum pressure drop values. But practically condition is reverse pressure drop due boat type element is minimum. This happens because the shape of the element body is not considered during thermal calculations. That's why it is very difficult to predict the pressure drop across the filter inlet and outlet is difficult by a theoretical method due to shape variation of the strainer.

One of the most reliable methods of calculating pressure drop in modern engineering age is Computational fluid dynamics (CFD) analysis.

## 2. CFD MODEL

The Y Filter is a versatile component for use as pre-filter in water systems. Y-type filters are commonly supplied for the water industry in accordance with ASME B 16.34 for casted versions, while for welded versions ASME Section VIII is widely used.

Most commonly used design is the Y type filter is with a cylindrical element which is discussed in the previous chapter thoroughly. To calculate the pressure drop across the filter Fluid flow is modelled for CFD analysis. CFD model is created using SolidWorks Software.

Three different geometries have modelled for 12-inch Filter, Existing Model, Modified Model-I and Modified Model-II in fully clean condition as shown in Figure 3, 4, and 5 respectively considered for the present analysis.

The Existing Model has a cylindrical type element. For analysis purpose model is divided into three sub-parts called inlet body, element, and the outlet body. To create well-developed flow here inlet pipe is extended to 1200 mm and outlet pipe extended to 1800mm long. Figure 4 shows the Modified Model-I.

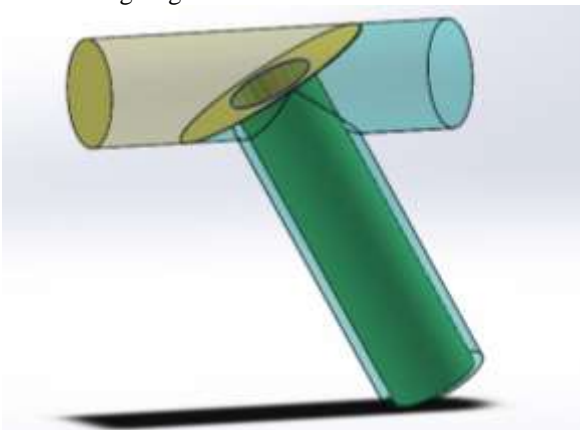


Fig. 3: Existing model

The body of Modified Model-I is kept remain the same as the existing model and changed are made in the shape of the filter element which is the heart of the filter. The new filter element is named as boat type element based on the shape. While modelling for the CFD analysis minor changes were made in shape of the element. Figure 3 shows the actual element shape. For analysis purpose model is divided into three sub-parts called inlet body, element, and the outlet body. To create well-developed flow here inlet pipe is extended to 1200 mm and outlet pipe extended to 1800mm long. Figure-4 shows the Modified Model-I.

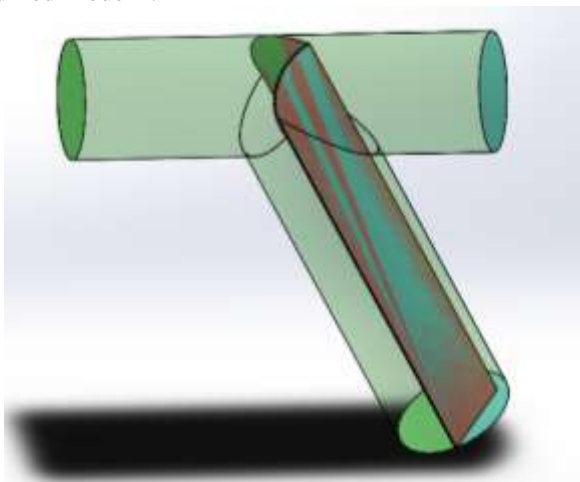


Fig. 4: Modified Model-I

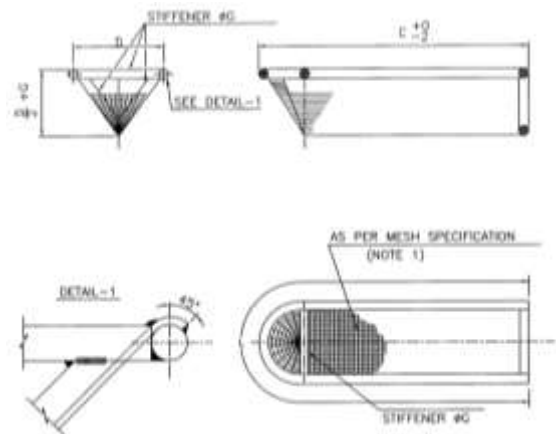


Fig. 5: Boat type element

Here in Modified model-II, changes were made in the body profile at just before the inlet to element and outlet to the element to achieve streamline flow to improve the pressure drop value. For analysis purpose model is divided into three sub-parts called inlet body, element, and the outlet body. To create well-developed flow here inlet pipe is extended to 1200 mm and outlet pipe extended to 1800mm long. Figure 6 shows the Modified Model-I.

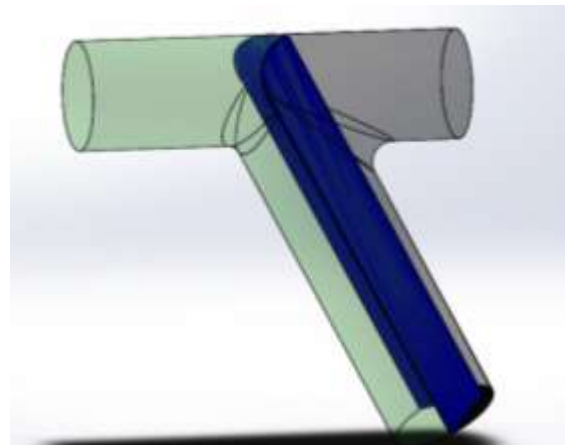


Fig. 6: Modified model-II

## 3. MESHING

In order to numerically solve the RANS equations from Chapter 4, it is necessary to discretize or partition a normally continuous medium into discrete volumetric cells, which consist of vertices and faces. A vertex is a point in space defined by a position vector as seen in Figure 7. A number of vertices can be used to define a feature curve or a face. A feature curve in its most basic terms consists of two vertices that define a line in two-dimensional space. A face defines a surface in three-dimensional space with four or more faces being used to define a three-dimensional cell. All of the volumetric cells combined are what is called a volume mesh.

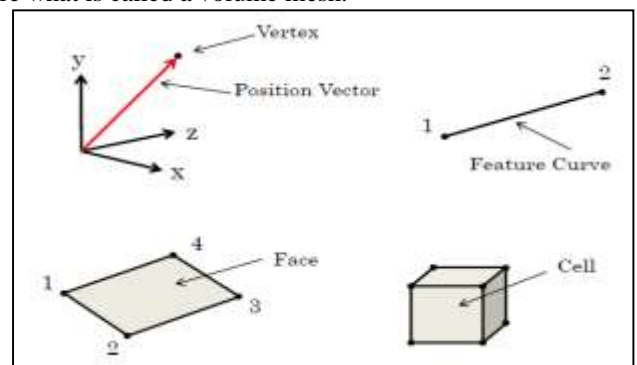


Fig. 7: Illustration of the individual components of a volume mesh

In a numerical simulation, a volume mesh represents the mathematical description of the space or geometry of the problem is solved. By solving the RANS equations using CFD, flow properties existent at each discrete volumetric cell such as the velocity, pressure, turbulence, etc. will attempt to simulate individually and as a whole. As the mesh is refined to better represent more discrete cells in the flow domain, the ability of CFD to simulate and predict the real-life conditions improves. However, the trade-off of a larger number of cells to compute is often undesirable due to a lack of computational resources. The meshing process in ANSYS involves creating some mesh continua for the continuum that one is attempting to model, selecting correct meshing models, making any changes to mesh sizing parameters and/or attributes globally and/or locally, setting volumetric controls, and running the surface and volume mesh generators. Checking the quality of the mesh by inspection and diagnostic tools usually follows as well as some iterations to get the correct sizing parameters for the specific simulation.

### 3.1 Geometry Meshing

In the present work, unstructured tetrahedral elements with high density near the element region, prisms at near-wall to capture the wall  $Y^+$  are created using ANSYS Fluent. Flow domain is extended to 6D on the upstream side and 8D on the downstream side to improve the flow field as shown in Figure 8 where sweep mesh is used.

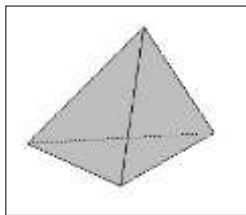


Fig. 8: Tetrahedron element

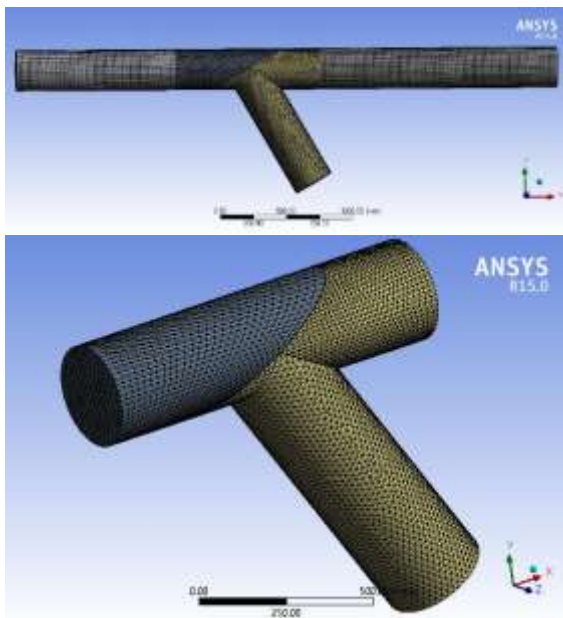


Fig. 9: Meshing view of existing model

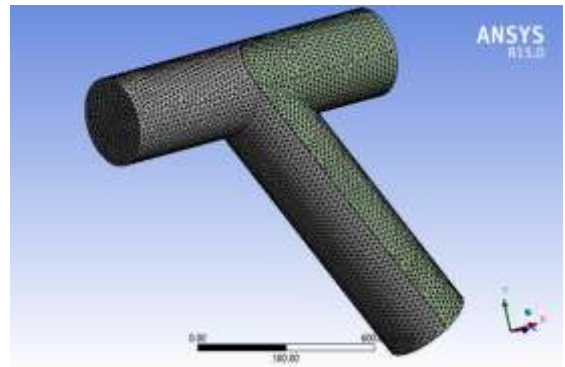
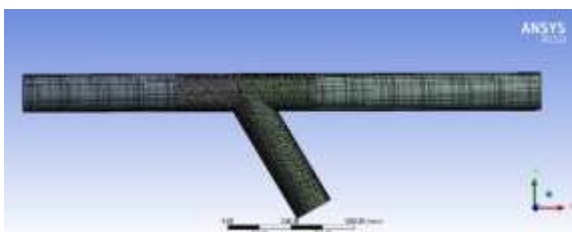


Fig. 10: Meshing view of modified model-I

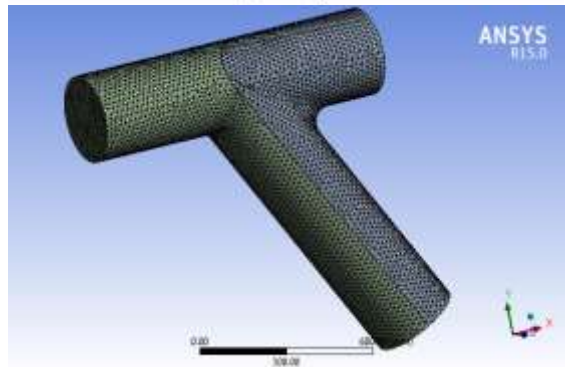
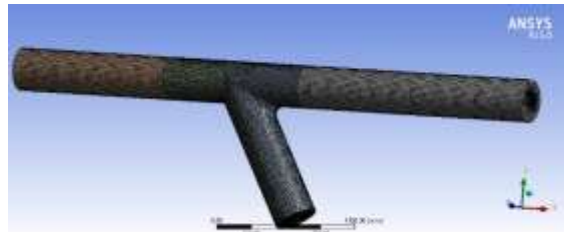


Fig. 11: Meshing view of modified model-II

## 4. BOUNDARY CONDITIONS

In three dimensions, boundaries are surfaces that completely surround and define a region. Each boundary has its own properties and can be given custom configurations such as meshing surface size, or how it should behave relative to other surfaces. The main boundary types chosen were the following: wall, an internal interface, velocity inlet, porosity and a flow outlet. These boundaries and their corresponding chosen surfaces for this study will now be discussed.

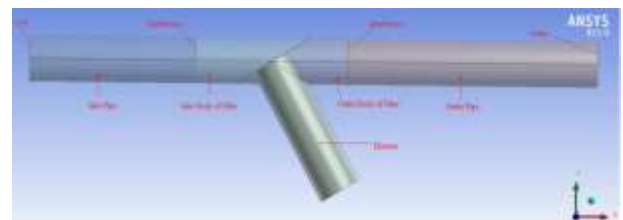


Fig. 12: Illustration of boundaries and components of the existing model simulations

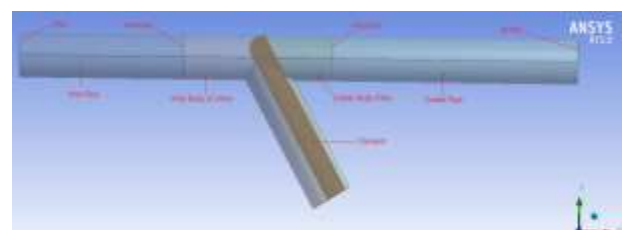
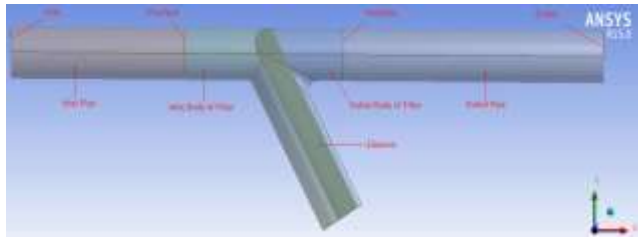


Fig. 13: Illustration of boundaries and components of the modified model-I simulations



**Fig. 14: Illustration of boundaries and components of the modified model-II simulations**

**4.1 Wall**

A wall boundary represents an impermeable surface. For simulations with a viscous flow such as this one, it also represents a no-slip boundary. All of the following surfaces were chosen as wall boundaries except the upstream inlet face, the downstream outlet face, and the interface connecting the downstream cylinder to the extruded cylinder portion as seen in Figure- 7.0.1. All valve faces were assumed to be smooth therefore required no modifications to surface roughness. All other wall roughness parameters were left as default.

**4.2 Velocity Inlet**

A velocity inlet boundary represents the inlet of a duct at which the flow velocity is known. The upstream cylinder inlet face was selected as such. For the velocity inlet boundary, the velocity must be specified by the user, as well as the turbulent dissipation rate and the turbulent kinetic energy when using the k- ε turbulence model, which was the case in this study.

**4.3 Flow Outlet**

The flow outlet boundary represents the outlet of a duct and can allow flow split fractions in which the user can specify the percentage of flow leaving multiple ducts. In this study, that value is set to unity for the downstream outlet face of the extruded cylinder. Additionally, flow properties such as velocity, turbulence qualities, etc. are forced to have zero gradients normal to the outflow face. In order to properly apply this boundary condition, the pipe length downstream from the installed butterfly valve must be long enough that the flow has become fully developed so as not to prematurely force the flow to a zero gradient condition.

**4.4 Fluid: Water Liquid**

The fluid for a CFD analysis is taken as liquid water whose properties are shown in Table 1.

**Table 1: Properties of liquid water**

Density (kg/m <sup>3</sup> )	998.2
Velocity (m/s)	4.6
Temperature (k)	288.16
Viscosity (kg/m-s)	0.001003

For instance, most flow manufacturers recommend installing their flow meters 10D to 20D downstream of any filter because swirling turbulent eddies generated by element largely disappear and the velocity flow profile returns to fully developed. In the study of how flow profiles changed for CFD simulation by forcing the zero gradient condition on the outlet for a filter simulation for different exit lengths. It was observed that in changing the exit length of the pipe downstream from 8D to 9D, a 2% difference was recorded. For this study, no significant differences were observed between simulation cases run initially with 10D exit lengths compared to 6D exit lengths. Consequently, a length of approximately 6D was used in order to simplify the flow model and computational requirements.

**4.3 Porous Media Conditions**

The porous media model can be used for a wide variety of single phase and multiphase problems, including flow through packed beds, filter papers, perforated plates, flow distributors, and tube banks. When you use this model, you define a cell zone in which the porous media model is applied and the pressure loss in the flow is determined via your inputs. Heat transfer through the medium can also be represented, subject to the assumption of thermal equilibrium between the medium and the fluid flow, here in our analysis it is not required. A 1D simplification of the porous media model termed the “porous jump,” can be used to model a thin membrane with known velocity/pressure-drop characteristics. The porous jump model is applied to a face zone, not to a cell zone, and should be used (instead of the full porous media model) whenever possible because it is more robust and yields better convergence. In our case, we are going with the momentum equation by modelling the element.

**4.4 Deriving Porous Media Inputs Based on Superficial Velocity, Using a Known Pressure Loss**

When you use the porous media model, you must keep in mind that the porous cells in ANSYS FLUENT are 100% open and that the values that you specify for  $1/\alpha_{ij}$  and/or  $C_{2,ij}$  must be based on this assumption. Suppose, however, that you know how the pressure drop varies with the velocity through the actual device, which is only partially open to flow. The following exercise is designed to show you how to compute a value for  $C_2$  which is appropriate for the ANSYS FLUENT model.

Consider a perforated plate which has 25% area open to flow. The pressure drop through the plate is known to be 0.5 times the dynamic head in the plate.

$$\Delta P = k \frac{\rho u_{25\%open}^2}{2} \tag{6}$$

To compute an appropriate value for  $C_2$ , note that in the ANSYS FLUENT model:

1. The velocity through the perforated plate assumes that the plate is 100% open.
  2. The loss coefficient must be converted into a dynamic head loss per unit length of the porous region.
- Noting item 1, the first step is to compute an adjusted loss factor,  $k'$ , which would be based on the velocity of a 100% open area:

$$\Delta P = k' \frac{\rho u_{100\%open}^2}{2} \tag{7}$$

or, noting that for the same flow rate,

$$k' = \frac{v_{25\%open}^2}{v_{100\%open}^2} \tag{8}$$

Noting item 2, you must now convert this into a loss coefficient per unit thickness of the perforated plate. Assume that the plate has a thickness of ‘t’. The inertial loss factor would then be

$$C_2 = \frac{k'}{t} \tag{9}$$

**Table 2: Inertial Resistance for Boat Type Element.**

S. No.	Inlet Velocity (V), m/sec	Adjusted loss factor $k'$	Inertial Resistance ( $C_2$ ), $m^{-1}$
1.	1.5	2.35	1468.62
2.	1.6	2.35	1468.62
3.	1.8	2.35	1468.62
4.	2.0	2.35	1468.62
5.	2.2	2.35	1468.62
6.	2.4	2.35	1468.62
7.	2.5	2.35	1468.62

**Table 3: Inertial Resistance for Boat Type Element.**

S. No.	Inlet Velocity (V), m/sec	Adjusted loss factor $k'$	Inertial Resistance ( $C_2$ ), $m^{-1}$
1.	1.5	2.35	1468.62
2.	1.6	2.35	1468.62
3.	1.8	2.35	1468.62
4.	2.0	2.35	1468.62
5.	2.2	2.35	1468.62
6.	2.4	2.35	1468.62
7.	2.5	2.35	1468.62

**Table 4: Pressure drop values using CFD**

S. No.	Inlet Velocity (V), m/sec	Pressure Drop ( $\Delta p$ ), $kg/cm^2$		
		Existing Model	Modified Model-I	Modified Model-II
1.	1.5	0.04773	0.01479	0.01408
2.	1.6	0.05667	0.02128	0.01537
3.	1.8	0.07054	0.02395	0.01800
4.	2.0	0.08601	0.02838	0.02191
5.	2.2	0.10129	0.03320	0.02502
6.	2.4	0.12288	0.03890	0.02673
7.	2.5	0.13299	0.04255	0.02842

**5. RESULTS**

All of the CFD simulations discussed were carried out using the criteria previously mentioned above. The flow fields generated by the simulations were studied, including visualizations of flow field streamlines, velocity vectors, and pressure fields. These visualizations are shown in Figure 15, 16, 17 and will be discussed accordingly. The pressure drops were also calculated and tabulated for comparison as shown in Tables 4.

**5.1 Visualization of the results**

A common characteristic of the simulated flow in all of the flow is the development and eventual dissipation of a pair of swirling vortices that form after passing around the element as seen in Figure 15 to 17.

Visualization of the flow field for the absolute pressure and the velocity vectors is presented in comparison with respect to velocity. If you see the figure 15 to 17 represents the pressure and velocity field for three models i.e. existing model, modified model-I, and modified model-II. Counter plots clearly represented that the pressure in the inlet body of the Existing model to more as compared to the modified models.

If we compare the Modified model-I and modified model-II for each velocity vector it is clearly seen that the flow path is get streamlined at the corner portions which helps in improvement of the pressure drop value.

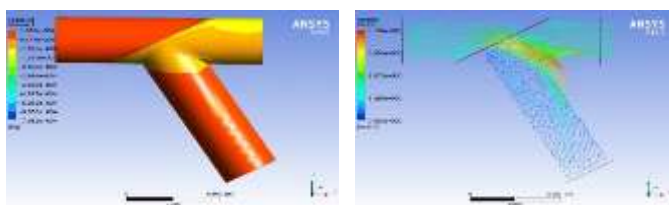


**Fig. 15: Pressure and velocity plot for existing model at 2.0 m/sec velocity**

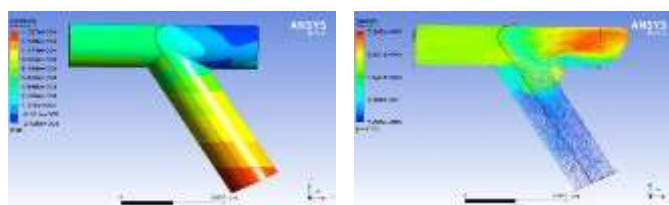


**Fig. 16: Pressure and velocity plot for modified model-I at 2.0 m/sec velocity**

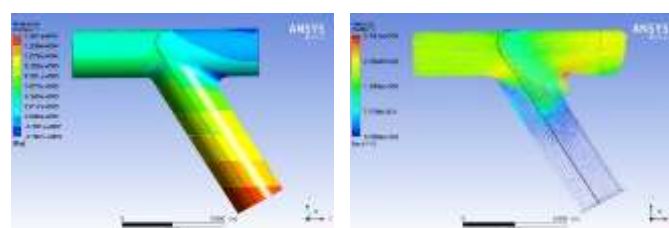


**Fig. 17: Pressure and Velocity Plot for Modified Model-II at 2.0 m/sec velocity**

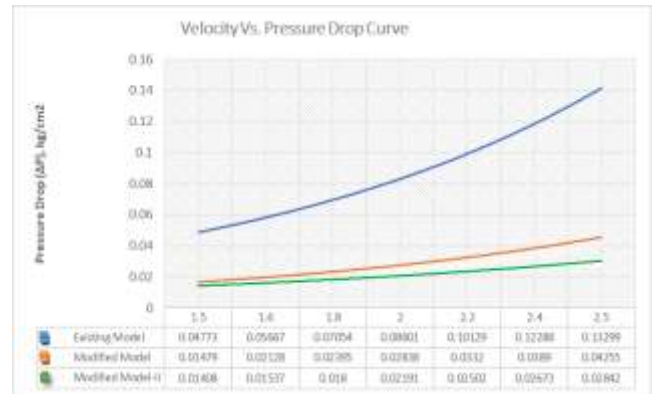


**Fig. 18: Velocity vs. Pressure Drop Curve**

**6. CONCLUSION**

CFD model of the filter is generated in SolidWorks and this model is imported to ANSYS Fluent for processing work. CFD analysis is carried out on the Y type strainer for different values of velocity that is for different flow rates. Numerical simulation is carried out to predict the flow behaviour across the flow filtering Y-strainer. Three different designs (Existing Model, Modified Model-I, Modified Model-II) are considered for the simulation. The following are the observations made:

- Flow behaviour is predicted in terms of pressure and velocity.
- It is seen that in Model-I, the flow path is diverted in a 60-degree angle to downwards side to enter inside the element. Also, there is an element retaining plate in between the straight flow path of the flow, which also acts as a barrier to the flow.
- In Modified model-I, it is seen that flow path remains to streamline because of removal of element retaining plate which helps in improvement of pressure drop. Approximately 67% improvement is seen after modification in modified model-I as compared to the existing model.
- A further modification was made in the body of modified Model-I keeping element shape and dimensions remain the same. Due to filleted corners, the pressure drop is improved in modified model-I.
- Approximately 75% improvement is seen after modification in modified model-II as compared to the Existing model.
- The present optimized design (Modified Model-II) helps in improving the flow field and pressure drop but increases manufacturing time.
- Further work on different size filter, different turbulence model, and validation with experimental data for the optimized design will add value to this work.

**6.1 Final Remarks**

- Computational fluid dynamics continues to be an impressive tool in helping model real-world problems.
- However, CFD can be used to give insight into the visualization of complex flows, and fluid flow problems one is attempting to solve.

- In this study, CFD was able to model the overall behavior of fluid flow for an incompressible fluid inside the filter at different velocities ranging from 1.5m/sec to 2.5 m/sec. If we compare the figure 3.3.2 and 8.1.22 it is seen that the more accurate and practical pressure drop is predicted by using CFD analysis.

## 7. REFERENCES

- [1] Partha Kundu, Vimal Kumar, Indra M. Mishra [1] in the paper titled "Experimental and numerical investigation of fluid flow hydrodynamics in porous media: Characterization of Darcy and non-Darcy flow regimes" reported in the Journal of Powder Technology.
- [2] Anurag Gupta Pushpdant Jain, Prabhsah Jain [2] (Dec. 2013) in the paper titled "Product Planning & Development of Y-Type Strainer Used in Thermal Power Plant and Process Plant" reported in the International Journal of Engineering Inventions, e-ISSN: 2278-7461, p-ISSN: 2319-6491 Volume 3, Issue 5 (December 2013) PP: 42-50.
- [3] Saeed Ovaysi<sup>1</sup>, Mohammad Piri<sup>2</sup> [3] (June 2010) in the paper titled "Direct pore-level modeling of incompressible fluid flow in porous media" reported in the Journal of Computational Physics by ELSEVIER, 229 (2010) 7456–7476.
- [4] Alexander Grahn<sup>1</sup>, Eckhard Krepper<sup>2</sup>, Frank-Peter Weiß<sup>3</sup> [4] (August 2010) in the paper titled "Implementation of a Pressure Drop Model for the CFD Simulation of Clogged Containment Sump Strainers" reported in the Journal of Engineering for Gas Turbines and Power by ASME, Vol. 132 / 082902-1.
- [5] A. Grahn<sup>1</sup>, E. Krepper<sup>1</sup>, S. Alt<sup>2</sup>, W. Kastner<sup>2</sup> [5] (April-2008) in the paper titled "Implementation of a strainer model for calculating the pressure drop across beds of compressible, fibrous materials" reported in the Nuclear Engineering and Design by ELSEVIER, 238 (2008) 2546–2553.
- [6] J. S. Andrade, Jr., U. M. S. Costa, M. P. Almeida, H. A. Makse and H. E. Stanley [6] (June 1999) in the paper title "Inertial Effects on Fluid Flow through Disordered Porous Media" reported in the Journal of Physics Review Letters by American Physical Society, Volume 82, 0031-9007/99/82(26)/5249(4).
- [7] K. Ann-Sofi Jonsson and Bengt T. L. Jonsson [7] (Sept. 1992) in the paper title "Fluid Flow in Compressible Porous Media: I: Steady-State Conditions" reported in the AIChE Journal Vol. 38, No. 9.
- [8] Chwan P. Kyan, Darshanlal T. Wasan, and Robert C. Kintner [8] (1970) in the paper title "Flow of Single-phase Fluids through Fibrous Beds" reported in the journal *Ind. Eng. Chem. Fundamen.*, 9 (4), pp 596–603.
- [9] Stephen Whitaker [9] (1969) in the paper title "Fluid Motion in Porous Media" reported in the journal of Industrial and Engineering Chemistry Vol. 61 No. 12.
- [10] B. F. Ruth [10] (July 1935) in the paper title "Studies in Filtration- IV. Nature of Fluid Flow through Filter Sept and Its Importance in the Filtration Equation" reported in the Journal of Industrial and Engineering Chemistry Vol. 27 No. 07.
- [11] B. P. Ruth with G. H. Montillon and R. E. Montonna [11] (Feb-1993) in the paper title "Studies in Filtration- II. Fundamental Axiom of Constant - Pressure Filtration" reported in the journal of Industrial and Engineering Chemistry Vol. 25 No. 02.
- [12] Reference book 1: Fluid Mechanics by K. L. Kumar.
- [13] Reference book 2: Fluid Mechanics by R. K. Bansal.
- [14] Perry Chemical Handbook.